NeuroImage 319 (2025) 121432

Contents lists available at ScienceDirect

NeuroImage

journal homepage: www.elsevier.com/locate/ynimg

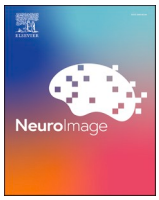

Frontoparietal network activity during a combined action observation and proprioceptive stimulation protocol reveals long-term plasticity in the primary motor cortex

Ambra Bisio [a], Costanza Iester [a], Monica Biggio [b], Laura Avanzino [a,c], Sabrina Brigadoi [d], Simone Cutini [d], Laura Bonzano [b,c,*], Marco Bove [a,c]

[a] Department of Experimental Medicine, University of Genoa, Genoa, Italy
[b] Department of Neuroscience, Rehabilitation, Ophthalmology, Genetics, Maternal and Child Health, University of Genoa, Genoa, Italy
[c] IRCCS Ospedale Policlinico San Martino, Genoa, Italy
[d] Department of Developmental and Social Psychology, University of Padova, Padua, Italy

ARTICLE INFO

Keywords:
Proprioception
Action observation
Transcranial magnetic stimulation
Functional near infrared spectroscopy
Plasticity

ABSTRACT

The aim of this study was to investigate changes in cortical hemodynamic activity within a frontoparietal network during the administration of an innovative action observation (AO) and proprioceptive stimulation (PS) protocol, and to examine whether this activity could predict the efficacy of the protocol in evoking M1 plasticity, reflected in significant long-term changes in M1 excitability. AO-PS was composed of 50 bursts of combined stimuli. Each burst consisted of five couples of AO and PS during which participants observed a video showing thumb opposition movements and simultaneously received a mechanical vibration on the extensor pollicis brevis muscle (stimulation frequency 80 Hz). During AO-PS, the hemodynamic activity was measured by means of functional Near-Infrared Spectroscopy. Recruitment curves were assessed using transcranial magnetic stimulation before, immediately, 30 and 60 min after AO-PS, to evaluate changes in M1 excitability. During AO-PS, a significant increase in oxyhemoglobin (HbO) concentration changes was found in the following Brodmann Areas (BA): left and right BA6, BA44, and BA43, left BA3, BA4, BA40 and BA7. The highest increment was found in the left BA4. In left BA7 and BA40 the time-to-peak in HbO concentration changes were reached significantly later than in the other BAs. On average, no significant changes were observed after AO-PS administration in M1 excitability, but HbO concentration changes in the left BA7 correlated with plasticity index. These findings highlight the involvement of sensorimotor and associative fronto-parietal regions during AO-PS. Additionally, the activity of the left BA7 revealed the plasticity induced by AO-PS in M1.

1. Introduction

Numerous studies have investigated how primary motor cortex (M1) excitability can be modulated through external cortical stimulation (Ziemann et al., 2008), peripheral stimulation (Kito et al., 2006; Naito and Ehrsson, 2001), and cognitive strategies such as action observation (Rizzolatti and Craighero, 2004) and motor imagery (Jeannerod, 2001). These approaches can induce both immediate, short-term increases in M1 activity (Fadiga et al., 1999, 1995; Naito et al., 1999) and more sustained, long-lasting effects (Huang et al., 2017; Siebner and Rothwell, 2003). Some protocols combine different types of stimulation to engage associative plasticity mechanisms (Suppa et al., 2017), for example. pairing cognitive strategies with peripheral stimulation to evoke motor cortex plasticity (Bisio et al., 2019, 2017, 2015; Bonassi et al., 2017; Kaneko et al., 2014). In a previous study (Bisio et al., 2019) we showed that the combination of action observation (AO) with kinesthetic illusion induced through proprioceptive stimulation led to a long-term increase in M1 excitability, when the directions of the observed and illusory movements were congruent and participants experienced a vivid illusory sensation of movement. This long-term increase in M1 excitability was interpreted as evidence of effectiveness of the protocol in inducing plasticity within M1. In a subsequent study (Bisio et al.,

* Corresponding author at: Department of Neuroscience, Rehabilitation, Ophthalmology, Genetics, Maternal and Child Health, University of Genoa, Largo Paolo Daneo, 3, 16132, Genoa, Italy.
E-mail address: laura.bonzano@unige.it (L. Bonzano).

https://doi.org/10.1016/j.neuroimage.2025.121432
Received 4 May 2025; Received in revised form 22 June 2025; Accepted 25 August 2025
Available online 25 August 2025

2021), we found a positive relationship between the individual's sensitivity to the combined protocol, measured as the increase in M1 excitability during protocol administration compared to rest, and the ability of the protocol to induce long-term changes in M1. These findings suggest that M1 excitability could serve as a potential individual marker of plasticity.

While the involvement of M1 in mediating the efficacy of the action observation–kinesthetic illusion protocol is thus established, it is also known that both AO and proprioceptive stimulation (PS) engage a broader frontoparietal network. This network includes sensorimotor regions as well as associative parietal and frontal areas (Henschke and Pakan, 2023; Romaiguère et al., 2003b). Increased activity in parts of this network, including the posterior parietal, premotor, and extrastriate cortices, has been observed when participants were exposed to congruent visual and proprioceptive input (Limanowski and Blankenburg, 2016). Therefore, other brain regions besides M1 are likely to contribute to and modulate the effects induced by an AO-PS protocol.

To address this issue, the present study employed functional Near-Infrared Spectroscopy (fNIRS) to investigate changes in cortical hemodynamic activity within a frontoparietal network during the administration of an innovative AO-PS protocol. Furthermore, it assessed whether these neural changes could predict the effectiveness of the protocol in inducing M1 plasticity, as assessed by means of Transcranial Magnetic Stimulation (TMS), in healthy young adults.

The novelty of the AO-PS protocol used in the present study lies in its greater ecological validity with respect to the previous one (Bisio et al., 2021, 2019). In earlier studies, participants observed a thumb opposition movement that was considerably longer in duration (10 s) than what typically occurs in a spontaneous movement (about 1 s). This extended timing was chosen to give enough time for the kinesthetic illusion to emerge. However, the kinesthetic illusion is highly subjective and varies across individuals, often requiring a prolonged period of stimulation, and consequently an extended display of the action, that does not correspond to its natural duration. For a future practical application of AO-PS as a tool to enhance cortical plasticity and motor learning in both rehabilitative and sports contexts, it is essential that the features of the observed actions closely mirror those encountered in real-life scenarios. Furthermore, from a neuroscientific point of view, previous studies showed that among the multiple features of the action that the observer must implicitly recognize, such as the biological law of motion (Bisio et al., 2014, 2010) and the motor repertoire (Calvo-Merino et al., 2005), the temporal characteristics play a crucial role in eliciting motor resonance (Avanzino et al., 2015; Lagravinese et al., 2017). Accordingly, in the AO-PS protocol proposed in the present study the observed action was aligned with the spontaneous duration of a thumb opposition movement, without being restricted to the conditions required to induce a kinesthetic illusion.

During AO-PS administration, we hypothesized the significant involvement of a brain network comprising sensorimotor and associative fronto-parietal regions. In line with previous studies, we also expected a significant and sustained increase in M1 excitability, potentially modulated by the activity of those brain regions most strongly engaged during AO-PS. To address these questions, hemodynamic concentration changes during AO-PS were measured using fNIRS, and M1 excitability was assessed through TMS before and after AO-PS.

2. Methods

2.1. Participants

A total of thirty healthy young adults were recruited for this study. All the participants were naïve to the purpose of the experiment and exhibited right-hand dominance, as determined by the Edinburgh Handedness Inventory (Oldfield, 1971). They reported no previous history of neurological disorders or orthopedic impairments. Participants had no contraindication to TMS. The study was conducted in accordance with the 2013 revision of the Declaration of Helsinki on human experimentation and was approved by the local ethics committee (Comitato Etico Territoriale - Liguria, N. 606/2023 - DB id 13,387, 18/12/2923). Written informed consent was obtained from all participants before participation in the study.

2.2. Experimental design

This study consisted in multiple sessions of evaluations to assess the effects on M1 excitability and on hemodynamic responses of a frontoparietal brain network induced by a protocol that combined AO with PS, namely AO-PS. Changes in M1 excitability were assessed by estimating recruitment curves using TMS at baseline (PRE), immediately after (POST0), and at 30 (POST30) and 60 (POST60) minutes following the AO-PS intervention. Hemodynamic responses were obtained by analyzing the time course of oxyhemoglobin (HbO) and deoxyhemoglobin (HbR) concentration during AO-PS, as measured with fNIRS (see paragraph 2.2.4). A graphical description of the experimental design is shown in Fig. 1.

2.2.1. Stimulation paradigm

The AO-PS stimulation paradigm consisted of 50 bursts of combined stimuli. Each burst was composed of 5 couples of AO and PS, each one lasting 1 s, interleaved by 1s-pause, for a total duration of 10 s. AO consisted in observing a video showing a thumb opposition movement towards the palm. Simultaneously, a proprioceptive stimulation was delivered using a mechanical vibrator (VB200; Vibrasens, Technoconcept) driven at 80 Hz with an amplitude of 80 % of the maximum (corresponding to 5 mm axial displacement) to activate muscle spindles (Roll et al., 1989; Roll and Vedel, 1982). Each burst was separated from the successive one by a jittered pause of 10–13 s. The total duration of the stimulation protocol was about 20 min. Before the administration of AO-PS, the experimenter asked participants to mentally rate the vividness of the illusory experience on a Likert scale from 0 (no illusory movement) to 10 (feeling of real movement). At the end of AO-PS administration, participants had to report the average vividness of the illusory movement.

2.2.2. fNIRS

A multichannel NIRS system (NIRSport 2, NIRx Medical Technologies, Berlin, Germany) was used to acquire the fNIRS signals and measure HbO and HbR concentration changes. The system consisted of 32 optodes, 16 LED illumination sources and 16 active detectors, which were placed on a soft black tissue cap (EasyCap, Germany) worn by the participant. Pairs of sources and detectors operating at two continuous wavelengths of near-infrared light (760 nm and 850 nm) generated 44 standard channels (3 cm) and 8 short-separation (SS) channels (8 mm). All channels were arranged to cover the prefrontal, sensorimotor and parietal areas through an fNIRS cap with labels according to the 10–10 EEG reference system. To choose the appropriate cap size, the participant's head circumference was measured. For precise placement, Cz was positioned halfway between the nasion and the inion, and between ear tragus points.

The Brodmann brain atlas in the fNIRS Optodes' Location Decider (fOLD) toolbox was used to establish the localizations of the channels (Zimeo Morais et al., 2018). The standard channels, their MNI coordinates, and the associated Brodmann Area (BA) are reported in detail in Table 1. A frequency of 10.2 Hz was chosen for the sampling.

2.2.3. TMS

TMS was used to assess changes in the excitability of the left M1, specifically in the region corresponding to the abductor pollicis brevis (APB) muscle. This muscle was selected because it is directly involved in both the observed and the illusory movements, and its excitability has been previously shown to be modulated by the combined application of action observation and proprioceptive stimulation (Bisio et al., 2021,

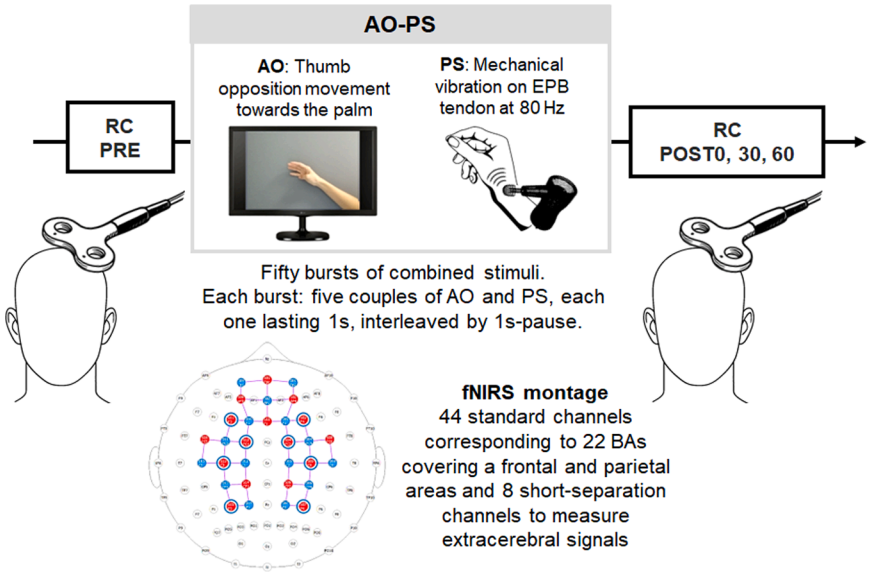

Fig. 1. Experimental design. A stimulation paradigm combining the observation of thumb opposition movements (Action Observation – AO) and simultaneous proprioceptive stimulation (PS) consisting in 80 Hz-mechanical vibration administered on the extensor pollicis brevis (EPB) muscle tendon of the right wrist. Changes in M1 excitability were assessed by estimating the recruitment curves (RC) using TMS at baseline (PRE), immediately after (POST0), and at 30 (POST30) and 60 (POST60) minutes following AO-PS. During AO-PS, fNIRS was used to evaluate oxyhemoglobin and deoxyhemoglobin concentration changes in a frontoparietal network.

2019). A single-pulse Magstim 200^2 stimulator (Magstim Co., Whitland, Wales, UK) connected to a figure-of-eight coil (70 mm wing diameter) was used. The coil was positioned tangentially on the scalp, with the handle pointing backward and laterally at a 45° angle to the sagittal plane. This orientation induces a posterior-to-anterior current in the brain and is known to produce the lowest motor threshold (Werhahn et al., 1994). To identify the optimal stimulation site for activating the right APB muscle, the coil was systematically moved in 0.5 cm increments in frontal, posterior, medial, and lateral directions around the assumed hand motor area. To ensure consistent coil positioning, once determined, the hotspot for the APB muscle and the coil orientation were marked on the scalp with an erasable marker. This enabled reliable repositioning of the coil, preserving both its location and orientation throughout the POST epochs. Although the procedure used in this study is well-established and has been consistently adopted in our previous work and in other studies, we acknowledge that neuronavigation systems allow achieving greater accuracy in coil positioning. While we did not use such a system, its absence may be considered a limitation of the present study.

Before starting the experiment, the stimulation intensity was individually adjusted for each participant to consistently evoke a motor evoked potential (MEP) with a peak-to-peak amplitude of approximately 1 mV in the resting APB muscle. Cortical excitability changes were tested by means of the recruitment curve (RC). RC was assessed by measuring peak-to-peak MEP amplitudes (mV) elicited at stimulus intensities ranging from 60 % to 140 % (in steps of 20 %) of the intensity able to evoke 1 mV in the APB muscle at rest (corresponding to 100 % step of the RC). Twenty trials were recorded at each TMS stimulus intensity, and the average MEP amplitude was taken as MEP size. A minimum time of 4 s was kept as TMS inter-stimulus interval during the RC construction. Stimulation intensities were kept constant throughout the entire experiment.

2.2.4. Electromyographic recording

MEPs were recorded using silver disc surface electrodes taped to the belly and tendon of the muscle. The ground electrode was placed at the elbow. Electromyographic (EMG) signals were digitalized, amplified, and filtered (20 Hz to 1 kHz) with a D360 amplifier (Digitimer) controlled by the Power 1401 acquisition interface (Cambridge Electronic Design Limited, Cambridge, UK), and stored on a personal computer for display and later offline data analysis. Each recording epoch lasted 400 ms, of which 100 ms preceded the TMS. Participants were constantly reminded to keep their hands relaxed during the whole experiment. The EMG signal was monitored visually by the experimenter and trials with background EMG activity were excluded from the analysis.

2.3. Data analysis

2.3.1. fNIRS

The fNIRS data was pre-processed for each participant with MATLAB (MathWorks, MA, USA) using custom scripts and functions from the Homer3 NIRS processing program (Huppert et al., 2009). Channels with a very low optical intensity or a low signal-to-noise ratio (SNR<2) were eliminated; the intensity data of the channels that survived were transformed into changes in optical density. A combination of the spline (p = 0.99) and wavelet (iqr=0.5) motion correction techniques were used to correct motion artifacts (Molavi and Dumont, 2012). Slow drifts and extremely high frequencies were eliminated by applying a band-pass filter (0.01–3 Hz). The hmrR_MotionArtifact function was then used to identify any remaining motion artifacts. A trial was excluded from additional analysis if motion artifacts were detected within −2 and 9 s after the task began. Each participant's age-dependent differential pathlength factor was calculated (Scholkmann and Wolf, 2013), and the modified Beer-Lambert law (Delpy et al., 1988) was then used to calculate the changes in HbO and HbR concentrations. The General Linear Model (GLM) method was used to retrieve the mean hemodynamic response function (HRF) for every task block, participant, and channel. An iterative weighted least squares method was used to solve the GLM (Barker et al., 2013). The temporal basis components of the HRF were a series of Gaussian profiles spaced 2 s apart and with a standard deviation of 1 s. For the HRF calculation, the block average interval was set between −2 and 20 s. To remove the physiological noise, for each standard channel, the most correlated SS channel was used as regressor in the GLM. Then, the HRF of channels belonging to the same BA were averaged thus obtaining the HRFs of 22 regions of interest (Table 1).

For each participant, and BA, the average of the HbO mean

Table 1
Description of the recording channels: optode placements based on the 10–10 system, MNI coordinates, hemisphere, Brodmann Areas (BA) and anatomical location.

Channel	Source label	Detector label	x	y	z	Hemisphere	BA	Anatomical location
1	C3	C5	−60	−18	37	Left	3,2,1	Postcentral gyrus
2	CP1	C1	−27	−36	71	Left	3,2,1	Postcentral gyrus
3	C3	C1	−42	−20	62	Left	4	Precentral gyrus
4	FC1	FC3	−38	12	55	Left	6	Superior frontal gyrus
5	FC1	C1	−26	−5	68	Left	6	Superior frontal gyrus
6	C3	FC3	−50	−3	50	Left	6	Superior frontal gyrus
7	CP1	P1	−24	−62	62	Left	7	Superior frontal gyrus
8	P3	P1	−32	−73	47	Left	7	Superior parietal lobule
9	FC1	F1	−23	26	56	Left	8	Superior frontal gyrus
10	AF3	F1	−23	52	32	Left	9	Middle frontal gyrus
11	F3	F1	−31	39	41	Left	9	Middle frontal gyrus
12	Fz	F1	−9	41	50	Left	9	Superior frontal gyrus
13	Fpz	Fp1	−12	67	0	Left	10	Medial frontal gyrus
14	AF3	AFz	−12	62	23	Left	10	Superior frontal gyrus
15	AF3	Fp1	−24	63	9	Left	10	Middle frontal gyrus
16	P3	CP3	−46	−61	46	Left	39	Inferior parietal lobule
17	C3	CP3	−52	−34	52	Left	40	Postcentral gyrus
18	CP1	CP3	−39	−48	60	Left	40	Inferior parietal lobule
19	FC5	C5	−62	−3	23	Left	43	Postcentral gyrus
20	F3	FC3	−45	25	41	Left	44	Middle frontal gyrus
21	FC5	FC3	−55	12	34	Left	44	Precentral gyrus
22	C4	C6	62	−20	37	Right	3,2,1	Postcentral gyrus
23	CP2	C2	28	−36	71	Right	3,2,1	Postcentral gyrus
24	C4	C2	42	−21	62	Right	4	Precentral gyrus
25	FC2	FC4	39	12	54	Right	6	Middle frontal gyrus
26	FC2	C2	27	−4	68	Right	6	Superior frontal gyrus
27	C4	FC4	52	−4	48	Right	6	Precentral gyrus
28	CP2	P2	25	−62	63	Right	7	Superior parietal lobule
29	P4	P2	33	−74	48	Right	7	Superior parietal lobule
30	FC2	F2	24	26	55	Right	8	Superior frontal gyrus
31	AF4	F2	22	52	33	Right	9	Superior frontal gyrus
32	F4	F2	30	40	41	Right	9	Middle frontal gyrus
33	Fz	AFz	2	50	39	Right	9	Medial frontal gyrus
34	Fz	F2	10	41	50	Right	9	Superior frontal gyrus
35	Fpz	Fp2	13	67	0	Right	10	Medial frontal gyrus
36	Fpz	AFz	1	64	14	Right	10	Medial frontal gyrus
37	AF4	Fp2	25	63	9	Right	10	Middle frontal gyrus
38	AF4	AFz	13	61	24	Right	10	Superior frontal gyrus
39	P4	CP4	46	−62	47	Right	39	Inferior parietal lobule
40	C4	CP4	53	−35	52	Right	40	Postcentral gyrus
41	CP2	CP4	39	−49	60	Right	40	Postcentral gyrus
42	FC6	C6	64	−5	22	Right	43	Postcentral gyrus
43	F4	FC4	44	25	40	Right	44	Middle frontal gyrus
44	FC6	FC4	56	12	33	Right	44	Precentral gyrus

hemodynamic responses in the range between 5 and 13 s after burst onset was computed. In addition, a time-to-peak analysis was conducted to provide new insights into neural dynamics as in a previous study (Iester et al., 2025).

2.3.2. Statistical analysis

The statistical analyses were performed with SPSS (Statistical Package for the Social Sciences, SPSS 20, Chicago, IL, USA). The effect size measures were presented through partial eta squared (η^2 value), with cut-off points of 0.10, 0.25, 0.40 representing a small, medium, and high effect, respectively (Cohen, 2013). The significance level was set at $p < 0.05$, unless otherwise specified.

fNIRS. Active BAs were defined as regions showing statistically significant positive changes in HbO concentration, identified using two complementary methods. A one-tailed *t*-test against zero was applied to each area. In the first approach, the resulting t-values were then converted to z-scores, and regions with z-score values greater than 1.96 (corresponding to the 97.5th percentile) were considered active. The

second method involved applying a false discovery rate (FDR) correction for multiple comparisons to the p-values obtained from the *t*-tests. Further statistical analyses were performed only on the BAs found to be active in at least one condition ($n = 10$).

HbO concentration changes of the active BAs were normally distributed according to the Shapiro–Wilk test. Repeated measure ANOVA was used to statistically compare HbO concentrations among the active BAs. In case of significant effects, Bonferroni post-hoc was used. Since the time-to-peak data were not normally distributed, the Friedman test followed by post-hoc analysis was used to assess differences in this variable among the active BAs.

To evaluate BA-to-BA task-based functional connectivity, Pearson's correlations were assessed considering the active BAs. Adjusted p-values were calculated using FDR correction to account for multiple comparisons.

TMS. The slope of the RC and the area under the curve (AUC) of the RC were computed to evaluate the relative changes in the rate of upper and lower motor neuron recruitment and cortical excitability (Turco and Nelson, 2021), respectively, from pre- to post- exposure to AO-PS. Slope values were obtained by applying a regression model to the linear part of the RC of each participant, namely from 80 % to 120 %. The AUC was calculated for each participant using the trapezoidal area method.

Both RC slope and AUC were not normally distributed according to the Shapiro–Wilk test. Friedmann tests were used to statistically compare slope and AUC values at the different testing epochs (TIME), namely before (PRE), immediately after (POST 0), 30 min after (POST30) and 60 min after (POST 60) AO-PS administration.

Correlation between fNIRS and TMS data. To unveil possible relationships between hemodynamic responses in the active BAs (according to the result of statistical analysis on fNIRS data) and the changes in slope and AUC values of the RC, plasticity indices were obtained as follows. RC slope and AUC values in POST epochs were normalized to their baseline values (PRE), and the percentage ratio with respect to PRE were calculated as (POST/PRE)*100 for each participant, at each evaluation time epoch. These values were averaged across evaluation time epochs, and the mean percent ratio of RC slope and AUC values were computed for each subject (Bisio et al., 2021, 2019). In particular, the formula here used was the following:

$$plasticity\ index = mean\left(\frac{POSTO}{PRE}+\frac{POST30}{PRE}+\frac{POST60}{PRE}\right)\times 100$$

Values above 100 indicate an increase in the plasticity index, whereas values below 100 reflect a decrease.

RC slope did not follow a normal distribution, as indicated by the Shapiro–Wilk test, whereas the AUC was normally distributed. Accordingly, Spearman's and Pearson's correlation analyses were used to examine the relationships between the RC slope and AUC with HbO concentration changes in the active BAs. Adjusted p-values were calculated using FDR correction to account for multiple comparisons.

We report in advance that a significant positive correlation was observed between HbO concentration changes in left (L) BA7 (L-BA7) and the plasticity index derived from the AUC. To further investigate this relationship, a follow-up analysis was performed where HbO concentration changes in L-BA7 were quantified during the first 20 bursts of AO-PS (BIN I) and the last 20 bursts (BIN II). A *t*-test was used to compare BIN I and BIN II. A follow-up correlation analysis (Pearson's correlation), with FDR correction for multiple comparisons, was then applied between the plasticity index and both BIN I and BIN II, aiming to clarify how changes in HbO concentration throughout AO-PS relate to M1 excitability modulation.

3. Results

Four participants were excluded from the analysis due to issues during fNIRS data acquisition that prevented successful data collection. Therefore, a total of 26 participants were included in the analysis. During AO-PS, at the end of AO-PS administration, participants reported a mean vividness of the illusory movement equal to mean±sd=6.29 ±1.88 out of a maximum of 10.

3.1. fNIRS

Ten out of the 22 BAs were found to be active with both methods used. Z-score values giving information about the spatial distribution of the significantly active BAs are graphically represented in Fig. 2A. HbO and HbR concentration changes are represented in Fig. 2B Detailed results are reported in the Supplementary materials.

Significant differences in HbO concentration changes among the active BAs were found ($F(9234)=7.33$, $p = 0.0002$, $\eta^2=0.22$) (Fig. 3A). Bonferroni post-hoc tests revealed that HbO concentration change in the L-BA4 was significantly higher than in the L-BA6 ($p = 0.008$), right (R) BA6 (R-BA6) ($p = 0.014$), L-BA44 ($p = 0.033$), R-BA44 ($p = 0.005$), L-BA3 ($p = 0.026$), L-BA40 ($p = 0.015$) and L-BA7 ($p = 0.008$). No differences emerged with respect to the L-BA43 and R-BA43.

The analysis of the time-to-peak revealed that active BAs in the posterior parietal cortex reached their peak concurrently, and later than other active BAs. Indeed, a significant effect of the BAs was found on the time-to-peak values ($\chi2(9)=79.62$, $p = 0.0002$) (Fig. 3B). Post-hoc revealed that the time-to-peak was reached significantly later in the L-BA 7 compared to the L-BA3 ($p = 0.015$), L-BA44 ($p = 0.034$), L-BA4 ($p = 0.047$), L-BA6 ($p = 0.016$), L-BA43, R-BA6 and R-BA43 (the latter three always $p < 0.0005$). Also, the time-to-peak of the L-BA40 was reached significantly later than those of the L-BA3 ($p = 0.037$), L-BA43 ($p = 0.001$), L-BA6 ($p = 0.04$), R-BA43 and R-BA6 (the latter two always $p < 0.0004$).

From the functional connectivity analysis, positive correlations were found among BAs located in frontal lobe, in parietal lobe, and between frontal and parietal regions. Results are reported in Table 2 and displayed in a correlation matrix in Fig. 4.

3.2. TMS

No significant effect of TIME was found on RC slope and AUC values. Data are shown in Fig. 5.

3.3. Correlation between fNIRS and TMS data

A significant positive correlation emerged between the plasticity index calculated on RC AUC values and HbO concentration changes in the L-BA7 ($R = 0.58$, $p = 0.02$) (Fig. 6A). This means that the higher HbO concentration changes in L-BA7, the higher the increased in MEP amplitude from PRE to POST AO-PS. Conversely, negative changes in HbO concentration correspond to a decrease in MEP amplitude. It is worth noting that plasticity index values ranged from 75 % to 166 %. Values above 100 % may suggest LTP-like plasticity, whereas values below 100 % may indicate LTD-like plasticity. No correlations were found between RC AUC values and HbO in the other BAs.

The comparison between HbO concentration changes between BIN I and BIN II revealed no significant difference. The result of the follow-up correlation analyses between HbO concentration changes and the plasticity index based on RC AUC values showed a significant positive correlation in BIN II ($R = 0.60$, $p = 0.004$), but not in BIN I (Fig. 6B).

No correlations were found between HbO concentration changes and plasticity index obtained from the RC slope values.

4. Discussion

During AO-PS administration significant increased HbO concentration changes were observed across several frontal and parietal cortical regions, specifically in the left BA4, BA3, BA7, BA40, as well as in both the left and right BA6, BA43, and BA44. Among those areas, the left BA4

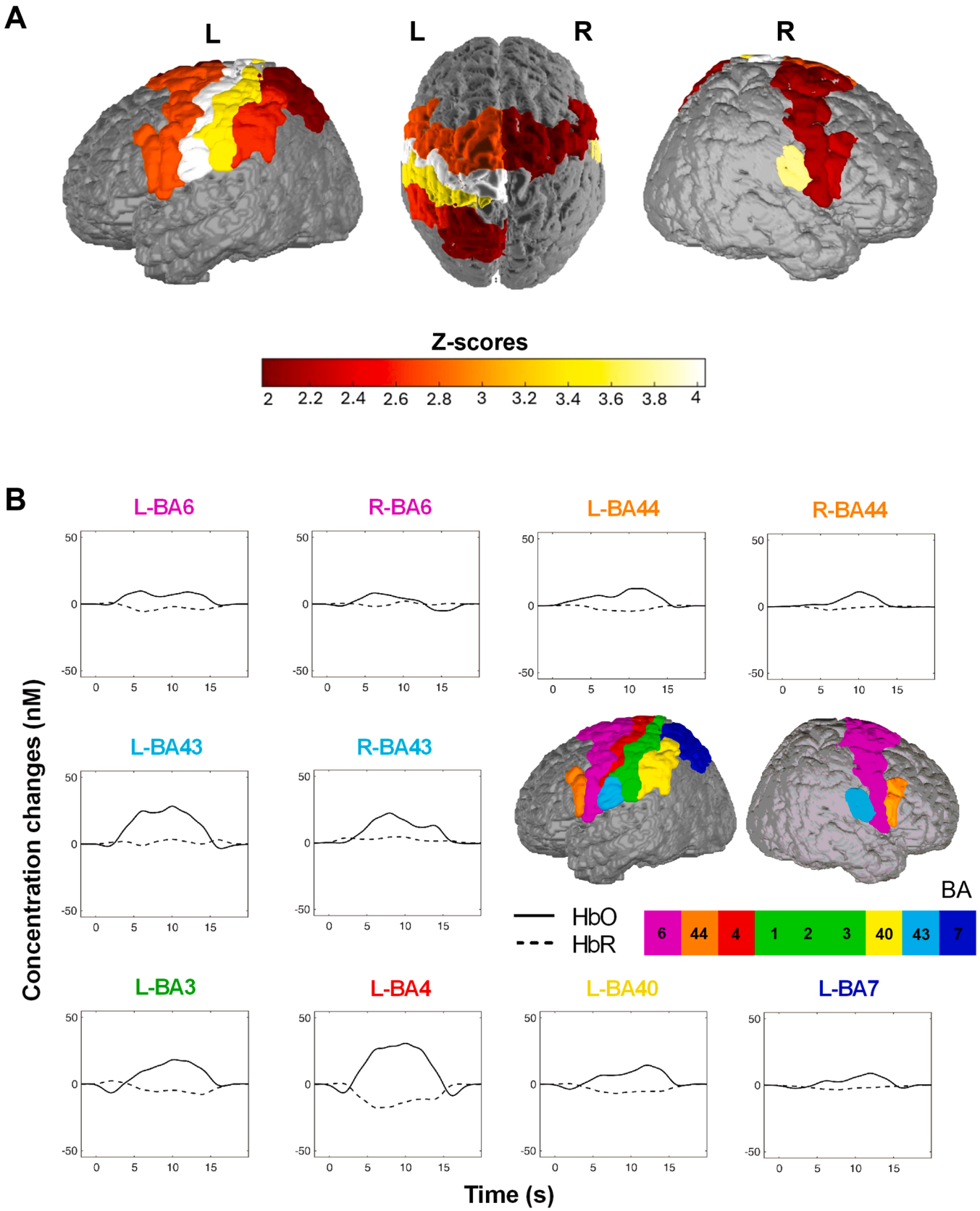

Fig. 2. fNIRS results. Brodmann Areas (BA) which resulted to be significantly activated in both left (L) and right (R) hemisphere during Action Observation-Proprioceptive Stimulation protocol according to z-scores values evaluation **(A)** and to the statistical significance appearing when comparing oxyhemoglobin changes with respect to zero (i.e., no change) **(B)**. The boxes show changes in oxyhemoglobin (HbO, continuous lines) and deoxyhemoglobin (HbR, dashed lines) concentration of these BAs.

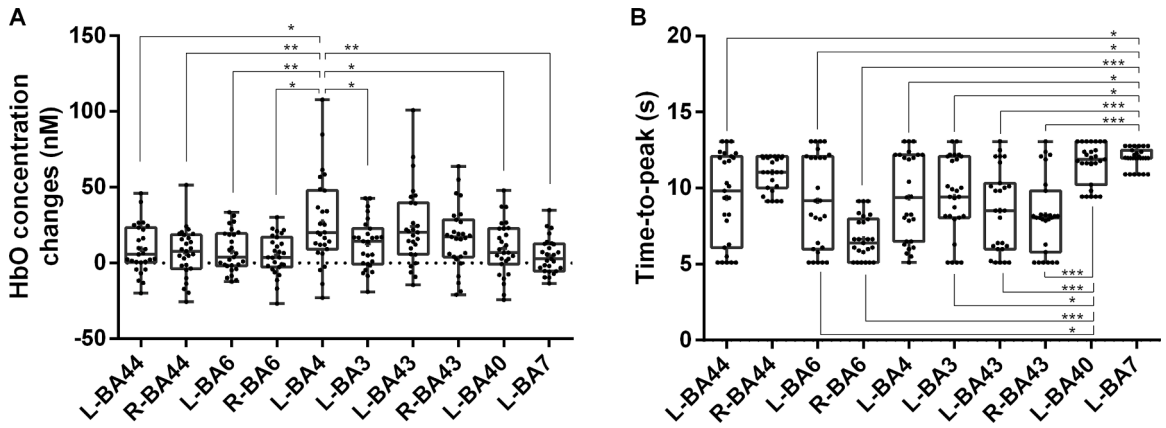

Fig. 3. fNIRS results. A) Changes in HbO concentration and **B)** time-to-peak of the active Brodmann Areas (BA). The box represents the inter-quartile ranges, the whiskers show the maximum and the minimum values and the horizontal central line the median value. Each circle indicates data from a single participant. * $p < 0.05$, ** $p < 0.01$, *** $p < 0.001$.

Table 2
Functional connectivity matrix. Result of the Pearson's correlation among HbO concentrations of the active brain Brodmann Areas (BA). Adjusted p-values with FDR correction are reported only for significant correlations.

BA	BA	R	p-value
L-BA44	L-BA6	0.80	< 0.00001
L-BA44	L-BA4	0.57	0.01
L-BA44	L-BA3	0.62	0.004
L-BA44	L-BA7	0.49	0.03
L-BA44	R-BA43	0.48	0.03
R-BA44	L-BA6	0.60	0.03
R-BA44	R-BA6	0.60	0.006
R-BA44	L-BA4	0.62	0.004
R-BA44	L-BA3	0.54	0.02
R-BA44	L-BA7	0.47	0.04
R-BA44	R-BA43	0.50	0.03
L-BA6	L-BA4	0.65	0.002
L-BA6	L-BA3	0.74	< 0.00001
L-BA6	L-BA40	0.46	0.04
R-BA6	L-BA3	0.48	0.03
R-BA6	L-BA40	0.46	0.03
L-BA4	L-BA3	0.79	< 0.00001
L-BA4	L-BA40	0.67	0.002
L-BA4	L-BA7	0.44	0.047
L-BA3	L-BA40	0.66	0.002
L-BA40	L-BA7	0.49	0.03

R – Pearson's correlation coefficient, L – left, R – right.

showed the highest increment. In the left BA7 and BA40 the time-to-peak in HbO concentration changes were reached significantly later than in the other BAs. Significant positive correlations were found among HbO concentration changes measured in areas within the frontal lobe, the parietal lobe, and between frontal and parietal lobes. On average, AO-PS did not induce significant changes in M1 excitability, as indicated by the slope and AUC of the RC. However, a significant positive correlation appeared between the plasticity index calculated on AUC and HbO concentration changes in the left BA7.

4.1. Fronto-parietal sensorimotor and associative areas active during AO-PS

Consistent evidence comes from scientific literature concerning the existence of an action-observation network that includes the ventral premotor cortex (BA44 and BA45), supplementary motor areas (BA6), the primary motor cortex (BA4), the somatosensory cortex (BA3), the inferior and superior parietal lobules (BA39, BA40, BA5 and BA7), and the superior temporal sulcus (BA21 and BA22) together with subcortical structures (Errante and Fogassi, 2020; Henschke and Pakan, 2023). Some of these areas are also actively engaged during proprioceptive stimulation that induces illusory movement perception, including the contralateral primary sensorimotor cortices, the supplementary motor area, and the posterior parietal cortex (Naito et al., 2002, 1999; Perasso et al., 2019; Romaiguère et al., 2003a). Therefore, the integration of visual and proprioceptive stimulation appears to be a plausible mechanism. This was shown by Limanowski & Blankenburg' study (Limanowski and Blankenburg, 2016), whose findings suggest that, when there is congruence between the two stimulations, namely, the position of the observed arm and the participant's own arm, a multimodal and reciprocal integration of the two motor representations into a unified percept may occur, leading to increased activation in the ventral premotor cortex, posterior parietal cortex, and the extrastriate body area. In the present study, as in previous ones (Bisio et al., 2021, 2019), congruency was achieved by presenting a thumb opposition movement while simultaneously eliciting an illusory perception of the same movement through proprioceptive stimulation. Based on previous results, the hypothesis was that AO-PS would have activated a fronto-parietal network including the ventral premotor cortex and posterior parietal cortex (Limanowski and Blankenburg, 2016), as well as M1 (Bisio et al., 2021). These hypotheses were confirmed by the present fNIRS findings, which revealed a significant increase in HbO concentration in bilateral BA44, L-BA7, L-BA40, and L-BA4.

In particular, the BA44, the Broca's area, constituting the frontal component of the human mirror neuron system, plays a pivotal role in critical domains, such as language and action (Binkofski and Buccino, 2006). In particular, it was found to be at the center of a brain network for the encoding of action intentions, either observed, heard or executed, and of action hierarchical structure, regardless of the modality (Fadiga et al., 2009). Since actions can also be encoded through their proprioceptive representation, referring to the prediction of expected feedback on body parts' position and velocity (Wolpert and Kawato, 1998), the significant increase observed in the present study may reflect the encoding of both the observed and the kinesthetically experienced action.

This multimodal encoding may also engage the parietal segment of the mirror neuron system, particularly BA40, located within the inferior parietal lobule and considered a core region of the posterior parietal cortex (PPC) (Rizzolatti and Rozzi, 2018). The PPC is a multimodal sensorimotor association area that integrates visual and somatosensory inputs and receives signals related to movement planning from the premotor and motor areas of the frontal lobe (Whitlock, 2017). Within PPC, BA40 is known to be responsive to a contralateral proprioceptive stimulation, thus playing a key role in kinesthesia (Kavounoudias et al., 2008; Romaiguère et al., 2003a). Alongside BA40, BA7, another key PPC region identified as significantly active in this study, contributes to

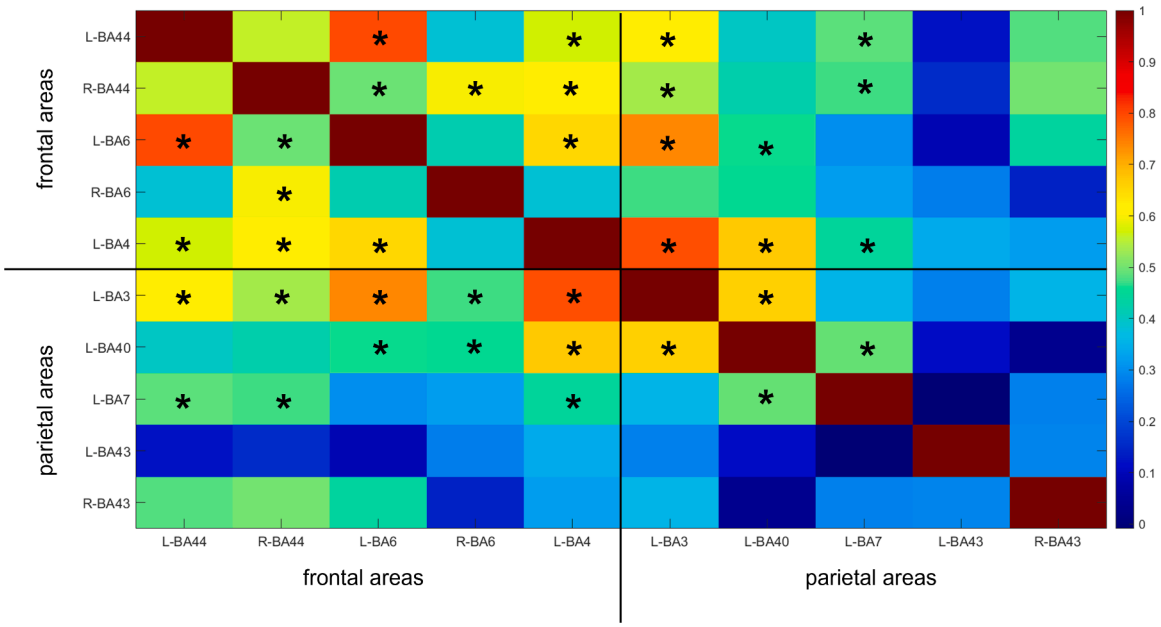

Fig. 4. Functional connectivity matrix. Color intensity indicates the strength of the correlation (see color bar), ranging from 0 (blue) to 1 (dark red). * marks statistically significant correlations ($p < 0.001$). Brodmann Areas (BA) belonging to frontal and parietal regions are grouped and separated by black lines.

maintaining an internal estimate of limb position. This internal model is continuously updated based on the congruence of dynamic inputs (Limanowski and Blankenburg, 2016). The observed activation of L-BA40 and L-BA7 may thus be interpreted as reflecting the continuous updating of the internal representation of body state, informed by converging inputs from action observation and proprioceptive stimulation. This continuous mechanism may be demanding in terms of neural resources required to sustain it, which could explain the delayed peak activation observed in L-BA40 and L-BA7 compared to other active BA.

A larger network than that shown in Limanowski and Blankenburg's study was found here active. Indeed, they reported the result of the contrast between congruent versus incongruent stimulation. Since the aim of the present study was to specifically investigate cortical activations during AO-PS to uncover potential relationships with M1 plasticity, we did not assess whether these activations were modulated by the congruency between the two stimulations. Therefore, we cannot rule out the possibility that the activation of L-BA4, L-BA3, as well as the bilateral BA6 and BA43, may be attributed either to a single type of stimulation or to the combined effect of both.

The significantly increased HbO concentration changes during AO-PS administration in the L-BA4 aligns with previous results from our group (Bisio et al., 2021), which showed that M1 excitability significantly augmented during combined congruent stimulation. Furthermore, intracortical recordings on monkeys showed that proprioceptive and visual inputs targeted a similar population of neurons within M1, supporting the hypothesis of a partial convergence of these signals in this region (Cross et al., 2024). However, whether this activation reflects a direct involvement of M1 in AO-PS or emerges from the integration of converging inputs from the Broca's area and PPC remains unclear based on the current data. In addition, L-BA4, together with L-BA3 and bilateral BA6, were reported by Kavounoudias and colleagues to be active during the mere proprioceptive illusion (Kavounoudias et al., 2008), as well as it is known that they are part of the action-observation network (Filimon et al., 2015). Moreover, the bilateral BA43, which constitute the secondary somatosensory cortex, were significantly active during AO-PS. Neurophysiological studies in both humans and monkeys have shown that these regions are involved in action prediction tasks (Abreu et al., 2012), the observation of actions involving touch (Sharma et al., 2018), and are also associated with proprioceptive stimulation (Bottini et al., 2001). Therefore, their activation during AO-PS might result from either type of stimulation or their combined effect.

4.2. Cortical network organization during AO-PS

Several of the brain regions appeared to function as a network during AO-PS, as evidenced by the functional connectivity analysis, which revealed significant positive correlations among the HbO concentration changes of BAs within and between the frontal and parietal lobes. Within the frontal lobe, L-BA4 showed significant correlations with both L-BA6, L-BA44 and R-BA44. Additionally, L-BA6 was significantly correlated with L-BA44 and R-BA44, while R-BA6 with R-BA44. These regions are all part of the frontal component of the mirror neuron system (Rizzolatti and Craighero, 2004), and their functional connectivity likely reflects its engagement during AO-PS. Within the parietal lobe, a significant correlation was observed between L-BA3 and L-BA40, likely reflecting the processing of proprioceptive signals. These signals are initially processed in L-BA3 and subsequently transmitted to the parietal associative area (L-BA40) for integration with other sensory inputs. A further significant correlation appeared between L-BA40 and L-BA7 two regions involved in the integration between the signals coming from the two sensory modalities (i.e., visual and proprioceptive).

The functional connectivity between the frontal and parietal lobes is expressed by the correlations between the HbO concentration changes of the L-BA3 with L-BA4, L-BA6, R-BA6, L-BA44, and R-BA44, as well as between L-BA7 with L-BA44 and R-BA44, presumably related to the activity of the dorsal action observation network consistently involved in AO (Filimon et al., 2015; Kilner, 2011). Significant correlations were also found between L-BA4 with L-BA7 and L-BA40. L-BA40 showed also significant correlation with L-BA6 and R-BA6. L-BA7 and L-BA40 are associative areas engaged in the multisensory integration of information from both AO and peripheral sensory inputs. This integrated information is transmitted to the frontal regions that may act as a hub for transforming the sensory percept into a motor percept potentially generating a sensorimotor resonance phenomenon (i.e., the vicarious activation of the sensorimotor system during AO) (Avenanti et al., 2010; DiGirolamo et al., 2019).

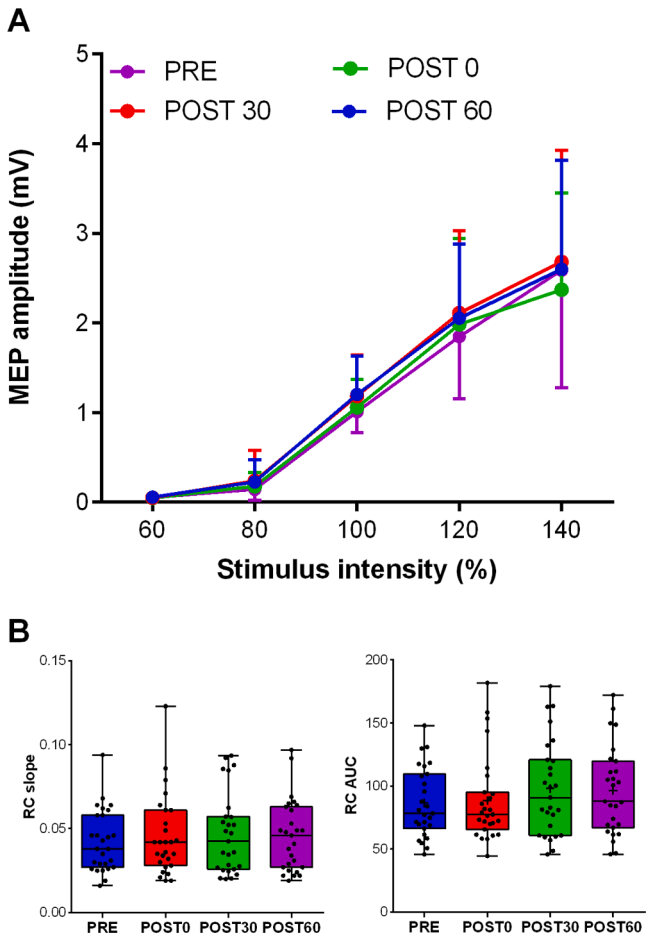

Fig. 5. TMS results. A) shows the recruitment curves (RC) evaluated before (PRE, blue), immediately after (POST0, red), 30 min after (POST30, green), and 60 min after (POST60, purple) the administration of the Action Observation – Proprioceptive Stimulation protocol. The group average motor evoked potential (MEP) amplitudes are represented as a function of TMS intensity. Data are expressed as means ± standard deviation. **B)** show the RC slope (left) and RC area under the curve (AUC, right) values. Each circle represents the data of a single participant. The black horizontal line represents the median; the box shows the interquartile range, and the whiskers extend to the minimum and maximum values.

4.3. Posterior parietal cortex activity correlates with AO-PS-induced M1 excitability changes

Previous studies of our group showed that the combination of action observation and a proprioceptive stimulation, inducing an illusory perception of movement congruent with that observed, evoked a LTP-like plasticity in M1 (Bisio et al., 2021, 2019). In the present study this result was not confirmed. Indeed, on average, no changes were observed in both RC slope and AUC values after AO-PS administration, suggesting that, on average, AO-PS failed to induce LTP-like plasticity in M1. The reason likely relies on the fact that the protocol we proposed was different from that already published. As explained in the Introduction (paragraph 1), the focus of this protocol was not on the illusory movement evoked by AO-PS. Instead, we aimed for the stimulation features to resemble those of a real movement, mainly in duration, without being limited by the need to evoke a vivid perception of movement, but with a reasonable assurance of activating the Ia muscle fibers through mechanical vibration. It is worth noting that the average vividness reported by participants at the end of the AO-PS protocol was comparable to that reported in previously published studies. Nevertheless, unlike previously done, we did not monitor vividness during each burst of stimulation, but only at the end of AO-PS administration. Therefore, due to the limited precision of the method used to assess vividness, we cannot conclusively relate the absence of plasticity to the vividness levels reported. This may represent a limitation of the present study. Moreover, it cannot be ruled out that increasing the number of iterations, thereby extending the stimulation period, might have enhanced the efficacy of AO-PS in inducing plasticity.

Nevertheless, thinking that the novel AO-PS protocol completely failed to induce plastic changes in M1 of all the volunteers may be misleading. Hints come from the values of the plasticity index that were higher than 100 % in the 60 % of the participants. These results suggest that 60 % of the participants were responsive to AO-PS, as evidenced by the long-term increase in M1 excitability following its administration. In contrast, the remaining 40 % showed values below 100 %, namely a decrease of M1 excitability after AO-PS administration. This interpretation is further supported by the significant positive correlation observed between the plasticity index and the HbO concentration changes in L-BA7, a region of the superior parietal lobule. This analysis suggests that increased HbO concentration changes during AO-PS were accompanied by a long-term increase in M1 excitability, while reductions in HbO concentration changes were associated with long-term decreases in excitability.

The L-BA7 has been proposed to play a role in representing the self within the surrounding space, particularly in projecting the body into the environment (Medendorp and Heed, 2019). If the environment includes a moving hand, one could speculate that this process involves merging the illusory movement of one's own hand with the observed movement of the external hand. In this regard, BA7 has been suggested to contribute to cross-modal plasticity following sensory loss, allowing intact sensory modalities to compensate for the deprived sense (Gilissen and Arckens, 2021). It can be speculated that this compensatory mechanism is also engaged when sensory functioning is intact, but an expected sensory input is absent. AO activates a neural network that largely overlaps with that involved in actual movement execution. What critically distinguishes AO from real movement is the absence of sensory feedback, as the individual does not physically move. Thus, AO can be conceived as an action deprived of its sensory consequences. Under these conditions, a mechanism of cross-modal plasticity may be recruited to compensate for the lack of proprioceptive input during AO. In the present case, such a mechanism may have facilitated the association between AO and PS, ultimately promoting an increase in M1 excitability in participants showing strong involvement of L-BA7, an effect that might indicate the occurrence of LTP-like plasticity. Consistent with this interpretation, a decrease in HbO concentration changes in L-BA7 was associated with a reduction in M1 excitability from PRE to POST, which may suggest the involvement of LTD-like plasticity mechanisms.

The existence of this positive correlation may inform future applications in rehabilitation and sports settings. In particular, the results of the follow-up correlations, showing a significant positive relationship between AUC plasticity index and HbO concentration changes assessed in the last bursts of AO-PS administration, suggest that the way hemodynamic concentration changes in L-BA7 evolves from the beginning (BIN I) to the end (BIN II) of AO-PS is what correlates with the efficacy of AO-PS to induce long-term modifications in M1 excitability. This results could support the use of AO-PS as an adjunct to conventional treatment or training, helping practitioners identify suitable candidates, namely, individuals who exhibit increased oxyhemoglobin demand in L-BA7 during AO-PS (as well as in M1, as previously reported (Bisio et al., 2021)). Thus, fNIRS data may serve as a biomarker to identify individuals potentially responsive to AO-PS, through real-time monitoring of HbO concentration changes in L-BA7 during protocol administration. Those individuals with positive HbO concentration changes would be those potentially responsive to AO-PS.

It should be noted that, at the present stage, the correlation observed between hemodynamic response in L-BA7 and the plasticity index

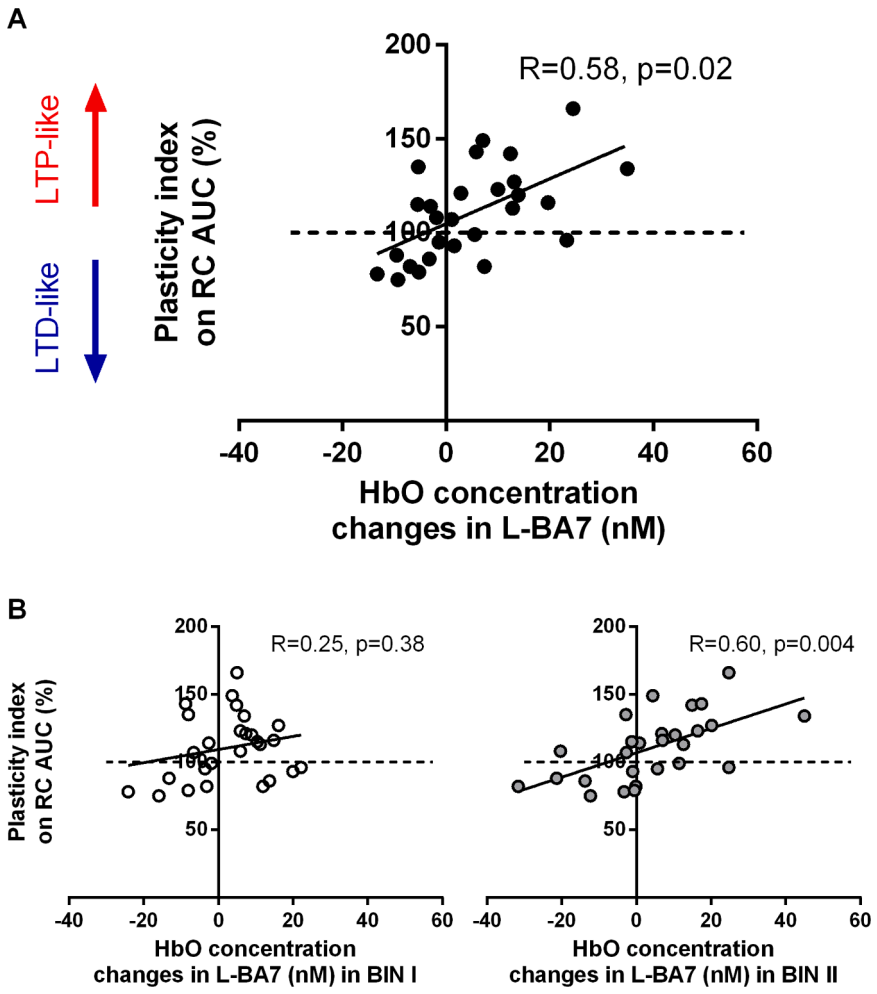

Fig. 6. Correlation between the plasticity index and HbO concentration changes in the left (L) BA7 during the whole stimulation (A) and in the first (left) and last (right) 20 bursts of Action Observation – Proprioceptive stimulation (AO-PS)**.** Circles display data from a single participant. The dashed horizontal line indicates no changes after the protocol administration. Y-axis shows the plasticity index calculated on the area under the curve (AUC) of the recruitment curve (RC). Values higher than 100 indicate an increase in the plasticity index suggesting that long-term potentiation (LTP-) like plasticity occurred, whilst values lower than 100 indicate a decrease, indicative of long-term depression (LTD-) like plasticity. The continuous line represents the linear regression model. Pearson's correlation coefficient and p-value are reported.

cannot be interpreted as evidence of a causal relationship. Future studies, with larger sample sizes, are necessary to test the causal relationship between cortical hemodynamic changes during AO-PS and subsequent changes in M1 excitability.

5. Conclusion

For the first time, this study sheds light on the involvement of sensorimotor and associative fronto-parietal regions during a protocol combining AO and PS. Furthermore, the positive correlation between hemodynamic changes in L-BA7 during AO-PS and subsequent M1 excitability suggests that fNIRS parameters may serve as biomarkers to identify individuals likely to benefit from AO-PS, an information useful for practitioners in both rehabilitation and sports settings.

Data and code availability statement

The data that support the findings of this study are available from the corresponding author upon request.

CRediT authorship contribution statement

Ambra Bisio: Writing – original draft, Visualization, Methodology, Investigation, Funding acquisition, Formal analysis, Data curation, Conceptualization. **Costanza Iester:** Writing – original draft, Visualization, Validation, Software, Methodology, Formal analysis, Data curation. **Monica Biggio:** Writing – review & editing, Investigation. **Laura Avanzino:** Writing – review & editing, Methodology. **Sabrina Brigadoi:** Writing – review & editing, Validation, Methodology. **Simone Cutini:** Writing – review & editing, Validation, Methodology. **Laura Bonzano:** Writing – review & editing, Validation, Methodology, Funding acquisition. **Marco Bove:** Writing – review & editing, Validation, Supervision, Methodology, Funding acquisition, Data curation, Conceptualization.

Declaration of competing interest

The authors declare that they have no known competing financial interests or personal relationships that could have appeared to influence the work reported in this manuscript.

Acknowledgments

Funded by the European Union - NextGenerationEU and by the Ministry of University and Research (MUR), National Recovery and Resilience Plan (NRRP), Mission 4, Component 2, Investment 1.5,

project “RAISE - Robotics and AI for Socio-economic Empowerment” (ECS00000035). The study has been also granted by the University of Genoa, Italy, through the competitive call “Bando Curiosity Driven 2021” supported by the Next Generation EU (D.R. n. 4093, 30/09/2022).

Supplementary materials

Supplementary material associated with this article can be found, in the online version, at doi:10.1016/j.neuroimage.2025.121432.

Data availability

Data will be made available on request.

References

Abreu, A.M., Macaluso, E., Azevedo, R.T., Cesari, P., Urgesi, C., Aglioti, S.M., 2012. Action anticipation beyond the action observation network: a functional magnetic resonance imaging study in expert basketball players. Eur. J. Neurosci. 35, 1646–1654. https://doi.org/10.1111/j.1460-9568.2012.08104.x.

Avanzino, L., Lagravinese, G., Bisio, A., Perasso, L., Ruggeri, P., Bove, M., 2015. Action observation: mirroring across our spontaneous movement tempo. Sci. Rep. 5, 10325. https://doi.org/10.1038/srep10325.

Avenanti, A., Sirigu, A., Aglioti, S.M., 2010. Racial bias reduces empathic sensorimotor resonance with other-race pain. Curr. Biol. 20, 1018–1022. https://doi.org/10.1016/j.cub.2010.03.071.

Barker, J.W., Aarabi, A., Huppert, T.J., 2013. Autoregressive model based algorithm for correcting motion and serially correlated errors in fNIRS. Biomed. Opt. Express. 4, 1366. https://doi.org/10.1364/boe.4.001366.

Binkofski, F., Buccino, G., 2006. The role of ventral premotor cortex in action execution and action understanding. J. Physiol. Paris 99, 396–405. https://doi.org/10.1016/j.jphysparis.2006.03.005.

Bisio, A., Avanzino, L., Biggio, M., Ruggeri, P., Bove, M., 2017. Motor training and the combination of action observation and peripheral nerve stimulation reciprocally interfere with the plastic changes induced in primary motor cortex excitability. Neuroscience 348, 33–40. https://doi.org/10.1016/j.neuroscience.2017.02.018.

Bisio, A., Avanzino, L., Gueugneau, N., Pozzo, T., Ruggeri, P., Bove, M., 2015. Observing and perceiving: a combined approach to induce plasticity in human motor cortex. Clin. Neurophysiol. 126, 1212–1220. https://doi.org/10.1016/j.clinph.2014.08.024.

Bisio, A., Biggio, M., Avanzino, L., Ruggeri, P., Bove, M., 2019. Kinaesthetic illusion shapes the cortical plasticity evoked by action observation. J. Physiol. 597, 3233–3245. https://doi.org/10.1113/JP277799.

Bisio, A., Biggio, M., Canepa, P., Faelli, E., Ruggeri, P., Avanzino, L., Bove, M., 2021. Primary motor cortex excitability as a marker of plasticity in a stimulation protocol combining action observation and kinesthetic illusion of movement. Eur. J. Neurosci. 53, 2763–2773. https://doi.org/10.1111/ejn.15140.

Bisio, A., Sciutti, A., Nori, F., Metta, G., Fadiga, L., Sandini, G., Pozzo, T., 2014. Motor contagion during human-human and human-robot interaction. PLoS ONE 9, e106172. https://doi.org/10.1371/journal.pone.0106172.

Bisio, A., Stucchi, N., Jacono, M., Fadiga, L., Pozzo, T., 2010. Automatic versus voluntary motor imitation: effect of visual context and stimulus velocity. PLoS ONE 5. https://doi.org/10.1371/journal.pone.0013506.

Bonassi, G., Biggio, M., Bisio, A., Ruggeri, P., Bove, M., Avanzino, L., 2017. Provision of somatosensory inputs during motor imagery enhances learning-induced plasticity in human motor cortex. Sci. Rep. 7. https://doi.org/10.1038/s41598-017-09597-0.

Bottini, G., Karnath, H.O., Vallar, G., Sterzi, R., Frith, C.D., Frackowiak, R.S.J., Paulesu, E., 2001. Cerebral representations for egocentric space: functional-anatomical evidence from caloric vestibular stimulation and neck vibration. Brain 124, 1182–1196. https://doi.org/10.1093/brain/124.6.1182.

Calvo-Merino, B., Glaser, D.E., Grèzes, J., Passingham, R.E., Haggard, P., 2005. Action observation and acquired motor skills: an FMRI study with expert dancers. Cereb. Cortex. 15, 1243–1249. https://doi.org/10.1093/cercor/bhi007.

Cohen, J., 2013. Statistical Power Analysis for the Behavioral Sciences. https://doi.org/10.4324/9780203771587.

Cross, K.P., Cook, D.J., Scott, S.H., 2024. Rapid online corrections for proprioceptive and visual perturbations recruit similar circuits in primary motor cortex. eNeuro 11. https://doi.org/10.1523/ENEURO.0083-23.2024.

Delpy, D.T., Cope, M., Van Der Zee, P., Arridge, S., Wray, S., Wyatt, J., 1988. Estimation of optical pathlength through tissue from direct time of flight measurement. Phys. Med. Biol. 33, 1433–1442. https://doi.org/10.1088/0031-9155/33/12/008.

DiGirolamo, M.A., Simon, J.C., Hubley, K.M., Kopulsky, A., Gutsell, J.N., 2019. Clarifying the relationship between trait empathy and action-based resonance indexed by EEG mu-rhythm suppression. Neuropsychologia 133. https://doi.org/10.1016/j.neuropsychologia.2019.107172.

Errante, A., Fogassi, L., 2020. Activation of cerebellum and basal ganglia during the observation and execution of manipulative actions. Sci. Rep. 10. https://doi.org/10.1038/s41598-020-68928-w.

Fadiga, L., Buccino, G., Craighero, L., Fogassi, L., Gallese, V., Pavesi, G., 1999. Corticospinal excitability is specifically modulated by motor imagery: a magnetic stimulation study. Neuropsychologia 37, 147–158. https://doi.org/10.1016/S0028-3932(98)00089-X.

Fadiga, L., Craighero, L., D’Ausilio, A., 2009. Broca’s area in language, action, and music. Ann. N. Y. Acad. Sci. 1169, 448–458. https://doi.org/10.1111/j.1749-6632.2009.04582.x.

Fadiga, L., Fogassi, L., Pavesi, G., Rizzolatti, G., 1995. Motor facilitation during action observation: a magnetic stimulation study. J. Neurophysiol. 73, 2608–2611.

Filimon, F., Rieth, C.A., Sereno, M.I., Cottrell, G.W., 2015. Observed, executed, and imagined action representations can be decoded from ventral and dorsal areas. Cereb. Cortex. 25, 3144–3158. https://doi.org/10.1093/cercor/bhu110.

Gilissen, S.R., Arckens, L., 2021. Posterior parietal cortex contributions to cross-modal brain plasticity upon sensory loss. Curr. Opin. Neurobiol. https://doi.org/10.1016/j.conb.2020.07.001.

Henschke, J.U., Pakan, J.M.P., 2023. Engaging distributed cortical and cerebellar networks through motor execution, observation, and imagery. Front. Syst. Neurosci. https://doi.org/10.3389/fnsys.2023.1165307.

Huang, Y.Z., Lu, M.K., Antal, A., Classen, J., Nitsche, M., Ziemann, U., Ridding, M., Hamada, M., Ugawa, Y., Jaberzadeh, S., Suppa, A., Paulus, W., Rothwell, J., 2017. Plasticity induced by non-invasive transcranial brain stimulation: a position paper. Clin. Neurophysiol. 128, 2318–2329. https://doi.org/10.1016/j.clinph.2017.09.007.

Huppert, T.J., Diamond, S.G., Franceschini, M.A., Boas, D.A., 2009. HomER: a review of time-series analysis methods for near-infrared spectroscopy of the brain. Appl. Opt. 48. https://doi.org/10.1364/AO.48.00D280.

Iester, C., Biggio, M., Brigadoi, S., Bisio, A., Brichetto, G., Cutini, S., Bonzano, L., Bove, M., 2025. Inferior parietal lobe activity reveals bimanual coupling and interference. Hum. Brain Mapp. 46, 1–12.

Jeannerod, M., 2001. Neural simulation of action: a unifying mechanism for motor cognition. Neuroimage 14, S103–S109. https://doi.org/10.1006/nimg.2001.0832.

Kaneko, F., Hayami, T., Aoyama, T., Kizuka, T., 2014. Motor imagery and electrical stimulation reproduce corticospinal excitability at levels similar to voluntary muscle contraction. J. Neuroeng. Rehabil. 11, 94. https://doi.org/10.1186/1743-0003-11-94.

Kavounoudias, A., Roll, J.P., Anton, J.L., Nazarian, B., Roth, M., Roll, R., 2008. Proprio-tactile integration for kinesthetic perception: an fMRI study. Neuropsychologia 46, 567–575. https://doi.org/10.1016/j.neuropsychologia.2007.10.002.

Kilner, J.M., 2011. More than one pathway to action understanding. Trends. Cogn. Sci. https://doi.org/10.1016/j.tics.2011.06.005.

Kito, T., Hashimoto, T., Yoneda, T., Katamoto, S., Naito, E., 2006. Sensory processing during kinesthetic aftereffect following illusory hand movement elicited by tendon vibration. Brain Res. 1114, 75–84. https://doi.org/10.1016/j.brainres.2006.07.062.

Lagravinese, G., Bisio, A., Ruggeri, P., Bove, M., Avanzino, L., 2017. Learning by observing: the effect of multiple sessions of action-observation training on the spontaneous movement tempo and motor resonance. Neuropsychologia 96, 89–95. https://doi.org/10.1016/j.neuropsychologia.2016.09.022.

Limanowski, J., Blankenburg, F., 2016. Integration of visual and proprioceptive limb position information in human posterior parietal, premotor, and extrastriate cortex. J. Neurosci. 36, 2582–2589. https://doi.org/10.1523/JNEUROSCI.3987-15.2016.

Medendorp, W.P., Heed, T., 2019. State estimation in posterior parietal cortex: distinct poles of environmental and bodily states. Prog. Neurobiol. https://doi.org/10.1016/j.pneurobio.2019.101691.

Molavi, B., Dumont, G.A., 2012. Wavelet-based motion artifact removal for functional near-infrared spectroscopy. Physiol. Meas. 33, 259–270. https://doi.org/10.1088/0967-3334/33/2/259.

Naito, E., Ehrsson, H., 2001. Kinesthetic illusion of wrist movement activates motor-related areas. Neuroreport 12, 3805–3809. https://doi.org/10.1097/00001756-200112040-00041.

Naito, E., Ehrsson, H., Geyer, S., Zilles, K., Roland, P., 1999. Illusory arm movements activate cortical motor areas: a positron emission tomography study. J. Neurosci. 19, 6134–6144.

Naito, E., Roland, P.E., Ehrsson, H., 2002. I feel my hand moving: a new role of the primary motor cortex in somatic perception of limb movement. Neuron 36, 979–988. https://doi.org/10.1016/S0896-6273(02)00980-7.

Oldfield, R.C., 1971. The assessment and analysis of handedness: the Edinburgh inventory. Neuropsychologia 9, 97–113. https://doi.org/10.1016/0028-3932(71)90067-4.

Perasso, L., Avanzino, L., Lagravinese, G., Giannini, A., Faelli, E.L., Bisio, A., Quartarone, A., Rizzo, V., Ruggeri, P., Bove, M., 2019. Boosting and consolidating the proprioceptive cortical aftereffect by combining tendon vibration and repetitive TMS over primary motor cortex. Neurol. Sci. 40, 147–154. https://doi.org/10.1007/s10072-018-3606-9.

Rizzolatti, G., Craighero, L., 2004. The mirror-neuron system. Annu Rev. Neurosci. 27, 169–192. https://doi.org/10.1146/annurev.neuro.27.070203.144230.

Rizzolatti, G., Rozzi, S., 2018. The mirror mechanism in the parietal lobe. Handb. Clin. Neurol. 555–573. https://doi.org/10.1016/B978-0-444-63622-5.00028-0.

Roll, J.P., Vedel, J.P., 1982. Kinaesthetic role of muscle afferents in man, studied by tendon vibration and microneurography. Exp. Brain Res. 47, 177–190. https://doi.org/10.1007/BF00239377.

Roll, J.P., Vedel, J.P., Ribot, E., 1989. Alteration of proprioceptive messages induced by tendon vibration in man: a microneurographic study. Exp. Brain Res. 76, 213–222. https://doi.org/10.1007/BF00253639.

Romaiguère, P., Anton, J.-L., Roth, M., Casini, L., Roll, J.-P., 2003a. Motor and parietal cortical areas both underlie kinaesthesia. Cogn. Brain Res. 16, 74–82. https://doi.org/10.1016/S0926-6410(02)00221-5.

Romaiguère, P., Anton, J.L., Roth, M., Casini, L., Roll, J.P., 2003b. Motor and parietal cortical areas both underlie kinaesthesia. Cogn. Brain Res. 16, 74–82. https://doi.org/10.1016/S0926-6410(02)00221-5.

Scholkmann, F., Wolf, M., 2013. General equation for the differential pathlength factor of the frontal human head depending on wavelength and age. J. Biomed. Opt. 18, 105004. https://doi.org/10.1117/1.jbo.18.10.105004.

Sharma, S., Fiave, P.A., Nelissen, K., 2018. Functional MRI responses to passive, active, and observed touch in somatosensory and insular cortices of the macaque monkey. J. Neurosci. 38, 3689–3707. https://doi.org/10.1523/JNEUROSCI.1587-17.2018.

Siebner, H., Rothwell, J., 2003. Transcranial magnetic stimulation: new insights into representational cortical plasticity. Exp. Brain Res. 148, 1–16.

Suppa, A., Quartarone, A., Siebner, H., Chen, R., Di Lazzaro, V., Del Giudice, P., Paulus, W., Rothwell, J.C., Ziemann, U., Classen, J., 2017. The associative brain at work: evidence from paired associative stimulation studies in humans. Clin. Neurophysiol. https://doi.org/10.1016/j.clinph.2017.08.003.

Turco, C.V., Nelson, A.J., 2021. Transcranial magnetic stimulation to assess exercise-induced neuroplasticity. Front. Neuroergonomics 2. https://doi.org/10.3389/fnrgo.2021.679033.

Werhahn, K.J., Fong, J.K., Meyer, B.U., Priori, A., Rothwell, J.C., Day, B.L., Thompson, P. D., 1994. The effect of magnetic coil orientation on the latency of surface EMG and single motor unit responses in the first dorsal interosseous muscle. Electroencephalogr. Clin. Neurophysiol. 93, 138–146. https://doi.org/10.1016/0168-5597(94)90077-9.

Whitlock, J.R., 2017. Posterior parietal cortex. Curr. Biol. https://doi.org/10.1016/j.cub.2017.06.007.

Wolpert, D.M., Kawato, M., 1998. Multiple paired forward and inverse models for motor control. Neural Networks 11, 1317–1329. https://doi.org/10.1016/S0893-6080(98)00066-5.

Ziemann, U., Paulus, W., Nitsche, M.A., Pascual-Leone, A., Byblow, W.D., Berardelli, A., Siebner, H.R., Classen, J., Cohen, L.G., Rothwell, J.C., 2008. Consensus: motor cortex plasticity protocols. Brain Stimul. 1, 164–182. https://doi.org/10.1016/j.brs.2008.06.006.